

Measuring Drug Metabolism Kinetics and Drug–Drug Interactions Using Self-Assembled Monolayers for Matrix-Assisted Laser Desorption-Ionization Mass Spectrometry

Lyndsey L. Anderson,^{†,⊥} Eric J. Berns,^{‡,⊥} Pradeep Bugga,[§] Alfred L. George, Jr.,^{*,†} and Milan Mrksich^{*,‡,§,||}

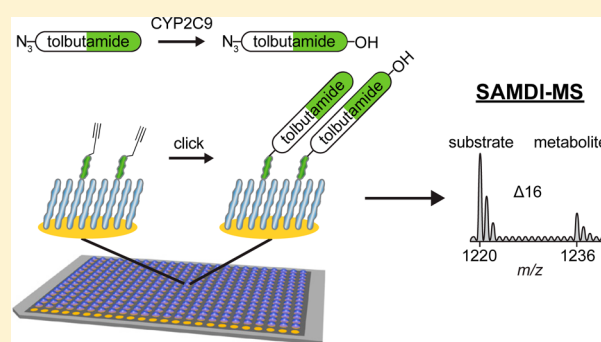
[†]Department of Pharmacology, Northwestern University Feinberg School of Medicine, Chicago, Illinois 60611, United States

[‡]Departments of Biomedical Engineering and [§]Chemistry, Northwestern University, Evanston, Illinois 60208, United States

^{||}Department of Cell and Molecular Biology, Northwestern University Feinberg School of Medicine, Chicago, Illinois 60611, United States

S Supporting Information

ABSTRACT: The competition of two drugs for the same metabolizing enzyme is a common mechanism for drug–drug interactions that can lead to altered kinetics in drug metabolism and altered elimination rates *in vivo*. With the prevalence of multidrug therapy, there is great potential for serious drug–drug interactions and adverse drug reactions. In an effort to prevent adverse drug reactions, the FDA mandates the evaluation of the potential for metabolic inhibition by every new chemical entity. Conventional methods for assaying drug metabolism (e.g., those based on HPLC) have been established for measuring drug–drug interactions; however, they are low-throughput. Here we describe an approach to measure the catalytic activity of CYP2C9 using the high-throughput technique self-assembled monolayers for matrix-assisted laser desorption-ionization (SAMDI) mass spectrometry. We measured the kinetics of CYP450 metabolism of the substrate, screened a set of drugs for inhibition of CYP2C9 and determined the K_i values for inhibitors. The throughput of this platform may enable drug metabolism and drug–drug interactions to be interrogated at a scale that cannot be achieved with current methods.



Drug–drug interactions are one of the primary causes of adverse drug reactions, which are responsible for approximately 100 000 deaths and an estimated \$30–130 billion in medical costs annually.^{1,2} Current methods for assaying cytochrome P450 (CYP450) drug metabolism and drug–drug interactions limit the extent and accuracy to which these phenomena can be characterized. Standard methods are time-consuming and labor-intensive or use probe substrates whose chemical structures deviate significantly from pharmaceutical substrates.^{3,4} Analytical high-pressure liquid chromatography (HPLC) and liquid chromatography–tandem mass spectrometry (LC–MS/MS) are low-throughput methods. As a result, the number of drug concentrations, time points, and probe substrates used to evaluate each CYP450 isoform is minimized to the extent that important information is missed and interactions are often generalized for all substrates metabolized by that isoform. An alternative approach using fluorescent probes offers greater throughput;³ however, the generic fluorescent probes differ significantly in chemical structure from the actual pharmaceutical substances. Since CYP450 inhibition is substrate-dependent, the use of fluorescent probes can result in IC_{50} values that vary as much as 50-fold from standard reference methods.⁵

A high-throughput platform capable of characterizing drug metabolism and drug–drug interactions using substrates closely resembling pharmaceutical substrates would enable more thorough and accurate investigation, potentially reducing the frequency of adverse drug reactions. Here we adapt a high-throughput technique using self-assembled monolayers for matrix-assisted laser desorption-ionization (MALDI)-mass spectrometry (SAMDI-MS) for assaying drug metabolism and to investigate drug–drug interactions for CYP2C9, an important isoform in the CYP2C subfamily, which is responsible for the metabolism of approximately 20% of clinically used drugs.⁶

We have developed SAMDI as a high-throughput method for analyzing chemical reactions, including enzyme activities.^{7–9} In one variation of this method, reactions are performed in solution, stopped, and then applied to self-assembled monolayers of alkanethiolates on gold, where the reactants and products undergo immobilization.¹⁰ The monolayers are functionalized with chemical moieties designed to capture the

Received: May 3, 2016

Accepted: July 28, 2016

Published: July 28, 2016

reactants and products and are terminated with tri(ethylene glycol) groups to prevent nonspecific adsorption.⁸ The monolayers are then treated with matrix and analyzed by MALDI mass spectrometry, during which dissociates the gold–thiolate bond is dissociated, releasing the molecules for time-of-flight (TOF) analysis. The relative areas of the peaks corresponding to the substrate and products can be used to quantify the extent of the reaction. Here, we report the successful adaptation of SAMDI for assaying CYP2C9 enzyme reactions.

EXPERIMENTAL SECTION

Reagents. All reagents were purchased from Sigma-Aldrich (St. Louis, MO) unless otherwise specified. Disulfides used to form self-assembled monolayers were purchased from ProChimia Surfaces (Sopot, Poland). Tris(3-hydroxypropyltriazolylmethyl)amine (THPTA) was purchased from Click Chemistry Tools (Scottsdale, AZ). Hydroxy-azido-tolbutamide was obtained from the ChemCore, part of the Center for Molecular Innovation and Drug Discovery, at Northwestern University. 2-Propyne-1-thiol was prepared according to the procedure in Schuster et al.¹¹

Synthesis of Azido-tolbutamide (azTolb). Reactions were performed in flame-dried glassware under a nitrogen atmosphere using dry, deoxygenated solvents passed over a column of activated alumina. *p*-Toluenesulfonyl isocyanate was purchased from Sigma-Aldrich. Thin-layer chromatography (TLC) was performed using EMD/Merck KGaA plates precoated with silica gel 60 F254 and visualized by UV fluorescence quenching. Silica gel (40–60 μm particle size) from Agela Technologies was used for flash chromatography. ¹H and ¹³C NMR spectra were recorded on a Varian Inova 500 and Bruker Avance III 500 (both at 500 MHz), respectively. Data for ¹H spectra is reported in terms of chemical shift relative to Me₄Si (δ 0.0 ppm) while that for ¹³C NMR is reported relative to CDCl₃ (δ 77.16 ppm). HRMS was acquired on an Agilent 6210A LC–TOF mass spectrometer using electrospray ionization (ESI).

The procedure from Landi et al. was used to prepare 3-azidopropylamine.¹² To a flame-dried flask (50 mL, pear-shaped), 3-azidopropylamine (8.87 mmol, 888 mg) in CH₂Cl₂ (18 mL) was added. After placing the flask in an ice bath, *p*-toluenesulfonyl isocyanate (1.63 mL, 3.06 mmol) was added. After 3-azidopropylamine was consumed by thin layer chromatography (TLC) analysis (~30 min), the reaction mixture was concentrated under vacuum. Purification via flash chromatography (75%–100% diethyl ether in hexanes eluent followed by 50:1 CH₂Cl₂/MeOH) yielded azido-tolbutamide (**1**) as a white solid (593 mg, 22%). ¹H NMR (500 MHz, CDCl₃) δ 9.27 (s, 1H), 7.80 (d, *J* = 8.3 Hz, 1H), 7.32 (d, *J* = 8.1 Hz, 1H), 6.68 (t, *J* = 5.9 Hz, 1H), 3.31 (q, *J* = 6.5 Hz, 1H), 3.27 (t, *J* = 6.7 Hz, 1H), 2.44 (s, 3H), 1.75 (quint, *J* = 6.7 Hz, 1H); ¹³C NMR (500 MHz, CDCl₃) δ 152.60, 144.92, 136.71, 129.98, 127.16, 49.03, 37.87, 28.85, 21.74; HRMS (ESI) *m/z* calculated for C₁₁H₁₄N₃O₃S [M – H][–], 296.0817; found, 296.0825. See the Supporting Information for NMR spectra.

Preparation of Self-Assembled Monolayers (SAMs). Stainless steel plates with dimensions matching standard MALDI plates (8 cm \times 12.3 cm) were cleaned with hexanes, ethanol, and water. An electron beam evaporator (Thermionics Laboratory Inc., Hayward, CA) was used to deposit a layer of titanium (5 nm at 0.02 nm/s) onto the plates. A mask with an

array of 2.8 mm circles laid out in a standard 384-well format was placed over the plates and the electron beam evaporator was used to deposit a second layer of titanium (5 nm at 0.02 nm/s) only on the exposed circles, followed by a layer of gold (35 nm at 0.05 nm/s). Plates were stored under vacuum until use. The plates were placed in a solution of two alkyl-disulfides in ethanol, 0.4 mM symmetric 11-carbon alkyl-disulfide terminated with tri(ethylene glycol) groups and 0.1 mM asymmetric alkyl-disulfide terminated with a maleimide group and a tri(ethylene glycol) group, for approximately 16 h. This is expected to produce monolayers with 10% of the alkanethiolates terminated with maleimide groups, based on previous work by the Mrksich group.¹³ In any event, the resulting maleimide density is sufficient for immobilizing probe substrates for quantitative analysis by SAMDI MS. The plates were removed, rinsed with ethanol, and placed in a 10 mM solution of hexadecylphosphonic acid in ethanol for 10 min. The plates were then rinsed with ethanol and dried with air. The 400 μM propyne thiol solution in ethanol was applied to each spot for 10 min, then rinsed with ethanol and dried with air. The plates were then used for immobilization of azTolb and hydroxyl-azTolb, described below.

CYP2C9 Reactions for SAMDI and HPLC. CYP2C9 metabolism of azTolb was performed in 15- μL reaction mixtures consisting of azTolb (25–1250 μM), 100 mM Tris buffer, pH 7.5, Supersomes purchased from Corning (Tewksbury, MA) containing human CYP2C9 and NADPH-P450 reductase. The CYP2C9 concentration (0.4 pmol/ μL) used in each reaction exhibited reaction velocities within the linear range when 200 μM tolbutamide was the substrate. Mixtures were preincubated at 37 $^{\circ}\text{C}$ for 5 min and the reaction was initiated by the addition of an NADPH-regenerating system (1.3 mM NADP⁺, 3.3 mM glucose-6-phosphate, 3.3 mM magnesium chloride, and 0.4 U/mL glucose-6-phosphate dehydrogenase). Reactions were then incubated at 37 $^{\circ}\text{C}$. Samples fated for analysis by SAMDI were terminated at various time points (0, 10, 15, 20, 25, and 30 min) by the addition of an equal volume of ice-cold methanol. Proteins were removed by centrifugation at 10 000g for 5 min, and the supernatant was used for analysis. AzTolb reactions for HPLC analysis were conducted the same as above with minor modifications. The 100- μL reactions were incubated at 37 $^{\circ}\text{C}$ for 60 min and terminated by the addition of 3 M HCl (25 μL). Samples were spiked with 10 mg/mL phenytoin, which was used as an internal standard. Extraction of hydroxyl-azTolb was achieved by vortex-mixing with diethyl ether (5 \times volume). The organic layer was isolated following centrifugation at 2000 rpm for 5 min and was evaporated by heating at 75 $^{\circ}\text{C}$. The residue was reconstituted in acetonitrile/water (1:1, v/v).

SAMDI-Mass Spectrometry. MALDI plates with alkyne-terminated monolayers were prepared as described above. CYP2C9 reaction samples were mixed 4:1 with a solution of “click” reagents -10 mM CuSO₄, 40 mM sodium ascorbate, and 20 mM THPTA. A volume of 3 μL of the sample mixture was dispensed onto each of 3 spots on the MALDI plate and incubated for 60 min at room temperature, then rinsed extensively with water and ethanol. Matrix (30–60 mg/mL 2,4,6-trihydroxyacetophenone in acetone) was applied to the monolayers on the MALDI plates and dried. Mass spectra were acquired from the plates with an Applied Biosystems 5800 MALDI-mass spectrometer. A 349 nm Nd:YAG laser was used as a desorption/ionization source. The accelerating voltage was 15 kV and the extraction delay time was 400–550 ns. All

spectra were acquired in positive reflector mode. A total of 900 laser shots (at a rate of 200 Hz) were applied while continuously moving the sample for the acquisition of each spectrum. The amount of hydroxy-azTolb formed was quantified by calculating the area under the curve for the substrate and product peaks at 1220 and 1236 m/z , respectively, using custom software. To account for potential differences in ionization efficiency between azTolb and hydroxy-azTolb, a standard curve was generated from varying ratios of azTolb and hydroxy-azTolb and this was used to determine percent conversion.

Analytical HPLC. Conversion of azTolb to hydroxy-azTolb was measured using a HPLC 9 Flexar Binary LC Pump Platform, Flexar UV-vis detector, and a Brownlee SPP C18 2.7- μm column (4.6 mm \times 150 mm; PerkinElmer, Waltham, MA). The mobile phase consisted of acetonitrile and 0.1% TFA in water (30:70, v/v) with a flow rate of 1 mL/min and detection at a wavelength of 220 nm. A volume of 50 μL of sample was injected per run.

Data Analysis. Kinetic parameters, K_M and k_{cat} , were calculated using nonlinear regression of the Michaelis–Menten equation in GraphPad Prism 6.07 (La Jolla, CA) to fit a plot of azTolb concentration against either velocity or initial reaction velocity determined by HPLC or SAMDI, respectively. The 95% confidence intervals (95% CI) for the K_M and k_{cat} values are reported in parentheses following the K_M and k_{cat} values. Initial reaction velocities were calculated from SAMDI time course data by fitting the data with least-squares linear regression to obtain slope values for each azTolb concentration. K_i values were determined from substrate-velocity curves determined in the presence of several concentrations of inhibitor. The competitive inhibitor or noncompetitive inhibitor model of enzyme inhibition that best fit the data was determined by GraphPad Prism, and the K_i value including the 95% confidence interval was calculated.

RESULTS AND DISCUSSION

Tolbutamide is a widely used oral hypoglycemic agent used to treat diabetes mellitus. This drug is metabolized by CYP2C9 to give a hydroxylated derivative¹⁴ and is recommended by the FDA for in vitro studies of drug development and interactions. To enable immobilization through copper-catalyzed azide–alkyne cycloaddition (CuAAC) click chemistry,¹⁵ we synthesized a derivative of tolbutamide (azido-tolbutamide; azTolb) with an azide moiety distant from the site of CYP2C9-catalyzed hydroxylation (Figure 1). In azTolb, the terminal methyl group of tolbutamide is replaced with an azide group, to minimize

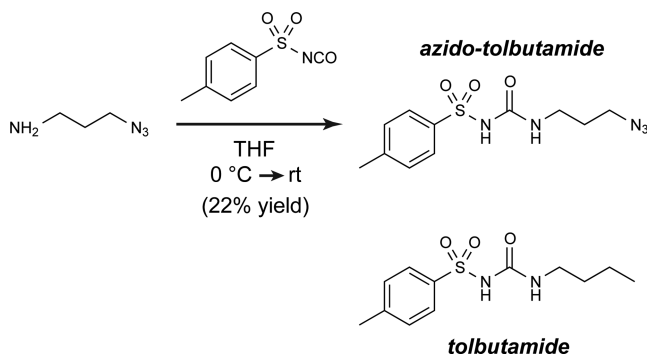


Figure 1. Synthesis of azido-tolbutamide (azTolb) and comparison to tolbutamide.

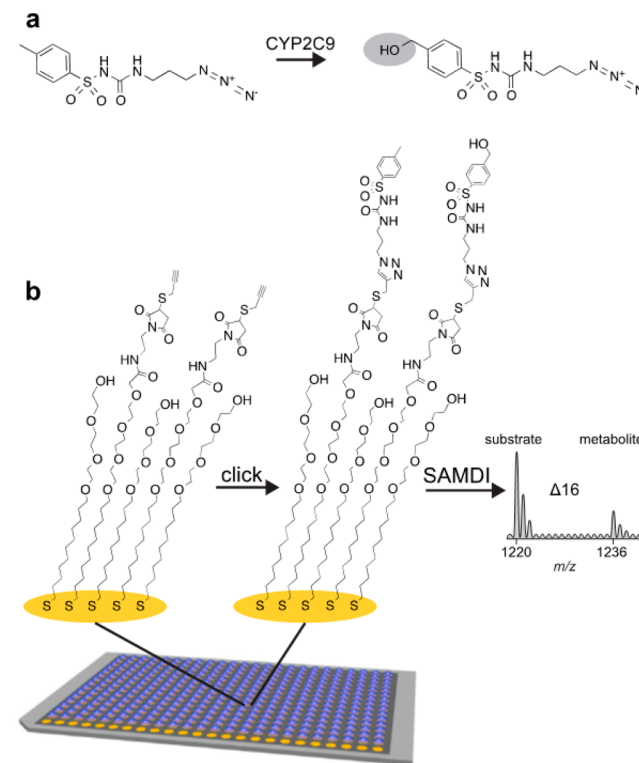
structural variation between the modified and original substrate. We chose to use CuAAC click chemistry because it is orthogonal to chemistries in biological systems and in drugs, thus enabling selective immobilization of the azide substrate in studies with microsomes and with additional drugs in drug–drug interaction experiments.

To determine whether modification of tolbutamide affected metabolism by CYP2C9, the kinetics of azTolb hydroxylation by CYP2C9 were analyzed by analytical HPLC and compared to that of tolbutamide. The K_M and k_{cat} of azTolb were 163 μM (95% CI, 67.7 to 258 μM) and 2.92 min^{-1} (2.45 to 3.39 min^{-1}), respectively, compared to 78 μM (34.2 to 122 μM) and 2.31 min^{-1} (2.01 to 2.60 min^{-1}) for tolbutamide. These results show that modification of the substrate did not result in significantly different K_M and k_{cat} values.

To evaluate the ability to characterize metabolism of azTolb by SAMDI, reactions with azTolb and CYP2C9 were carried out in solution. After termination of the reactions, the azTolb substrate and hydroxylated product were immobilized onto monolayers presenting terminal alkyne groups against a background of tri(ethylene glycol) groups with click chemistry (Scheme 1). The monolayers were prepared on plates having an array of 384 gold islands in the standard geometry. Following immobilization and application of matrix, SAMDI mass spectrometry was performed.

The amount of hydroxy-azTolb product was quantified by calculating the areas under the curves for the substrate and

Scheme 1. Illustration of the SAMDI-MS Assay for Azido-tolbutamide^a



^a(a) Chemical structures of azTolb and its CYP2C9 metabolite hydroxy-azTolb. (b) Reactions were applied to self-assembled monolayers, where a CuAAC click reaction gave covalent immobilization of azTolb and hydroxy-azTolb, which were then analyzed by SAMDI-MS.

product peaks, at 1220 and 1236 m/z , respectively (Figure 2a). Initial reaction velocities were calculated by measuring hydroxy-azTolb formation at several time points (Figure 2b).

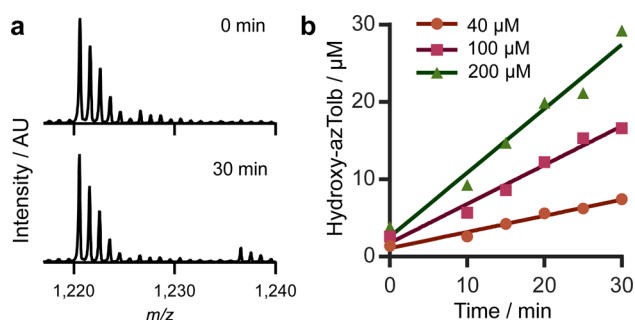


Figure 2. SAMDI assay of CYP2C9 metabolism of azTolb. (a) Representative spectra showing the results of an azTolb reaction at 0 and 30 min, showing the formation of hydroxy-azTolb (peak, 1236). (b) Average hydroxy-azTolb yield was plotted versus reaction time for three substrate concentrations to calculate initial reaction velocities, with $n = 3$ for each condition.

We determined the K_M and k_{cat} from nonlinear regression fits of plots of initial reaction velocities versus concentration of azTolb with the Michaelis–Menten equation (Figure 3). The

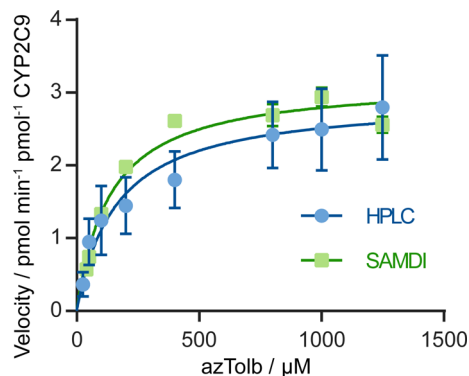


Figure 3. Michaelis–Menten kinetic plots of CYP2C9-catalyzed hydroxylation of azTolb determined by SAMDI and analytical HPLC. All data are expressed as mean \pm standard error of the mean, with $n = 3$ –6 per condition.

K_M determined for azTolb hydroxylation was 136 μM (70.9 to 200 μM) and the k_{cat} was 3.17 min^{-1} (2.76 to 3.58 min^{-1}). These values were not significantly different than those measured by HPLC (163 μM and 2.92 min^{-1}).

These experiments confirm that SAMDI is a robust and accurate method to assay CYP2C9 metabolism. Additionally, the throughput of the SAMDI assay, which can analyze approximately 1 000 reactions per hour,⁹ is more than 200-fold greater than HPLC, which takes approximately 15 min per run. Though the SAMDI approach requires an initial investment of time to synthesize the modified substrate, the remaining steps of monolayer formation, sample preparation, and click reactions can be performed so that high-throughput analysis is possible, with the potential to analyze thousands of samples per day. Indeed, a single drug analogue can be evaluated in combination with each of the approved drug molecules, amounting to tens of thousands of assays. The several days required to synthesize the analogue are insignificant when the total time to perform this number of assays by HPLC is considered.

As a proof-of-principle, we next demonstrated that SAMDI is capable of identifying drug–drug interactions. We screened the inhibitory potential of 12 compounds on CYP2C9 drug metabolism. These compounds included four known inhibitors of CYP2C9, four substrates, and four drugs that were not expected to inhibit CYP2C9 at the tested concentrations (Figure 4a). We first screened drugs at a concentration of 10

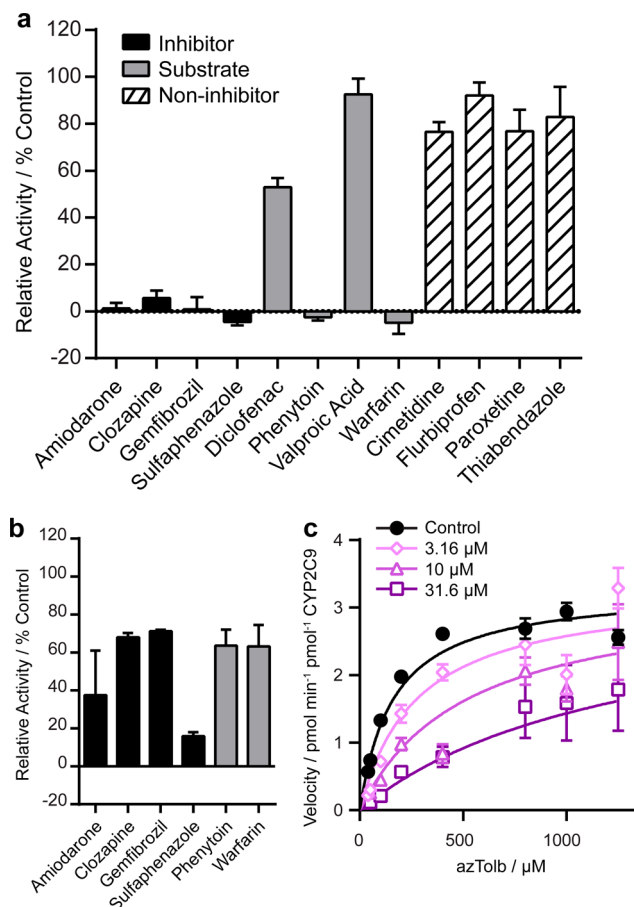


Figure 4. Drug–drug interaction screen. Relative CYP2C9 activity in the presence of drugs at (a) 10 μM or (b) 1 μM . (c) Representative plot for determining K_i values by testing three concentrations of inhibitor (diclofenac) across eight azTolb concentrations. All data are expressed as mean \pm standard error of the mean, with $n = 3$ per condition.

μM in combination with azTolb at its K_M (150 μM). The reactions were performed under the same conditions described above, except for the addition of the test drug. For each drug, we calculated the activity of CYP2C9 relative to the control and considered drugs that displayed greater than 40% reduction of enzyme activity to be inhibitors (here, 7 of the known inhibitors and substrates tested). Drugs exhibiting greater than 75% inhibition were subsequently screened at a concentration of 1 μM in order to determine the concentration range for K_i determination (Figure 4b).

The measured activities from these initial screens match the expectations based on reported K_i values for tolbutamide (right column of Table 1). For example, compounds with low reported K_i values, such as the inhibitor amiodarone or the substrate warfarin, resulted in nearly complete inhibition when screened at 10 μM (Figure 4a). Compounds with high K_i values, such as the substrate valproic acid or the drug

Table 1. K_i Values of Tested Compounds^a

	measured K_i azido-tolbutamide	published K_i tolbutamide
Amiodarone	1.1 μM (0.7–1.5)	0.69 μM ¹⁶
Clozapine	7.8 μM (3.4–12.1)	11.00 μM ¹⁶ 32 μM ¹⁷
Gemfibrozil	9.2 μM (2.7–15.9)	2.83 μM ¹⁶ 5.8 μM ¹⁸
Sulfaphenazole	0.8 μM (0.4–1.3)	0.22 μM ¹⁶ 0.669 μM ¹⁹
Diclofenac	4.5 μM (2.4–6.7)	0.76 μM ¹⁶ 6.0 μM ²⁰
Phenytoin	2.7 μM (1.3–4.1)	6.65 μM ¹⁶ 17 μM ¹⁷
Valproic Acid	>10 μM ^b	600 μM ²¹
Warfarin	1.3 μM (0.7–1.8)	2.13 μM ¹⁶
Cimetidine	>10 μM ^b	495 μM ²²
Flurbiprofen	>10 μM ^b	19.86 μM ¹⁶
Paroxetine	>10 μM ^b	>100 μM ²³
Thiabendazole	>10 μM ^b	33.09 μM ¹⁶

^aMeasured K_i values were obtained by SAMDI using azTolb as the probe substrate. Values in parentheses represent the 95% confidence interval. Published K_i values reported in the references were determined using tolbutamide as the probe substrate. ^bCompounds that did not reduce activity by greater than 40% when screened at 10 μM are designated as having an expected $K_i > 10 \mu\text{M}$.

thiabendazole resulted in almost no inhibition when screened at 10 μM (Figure 4a).

For each of the seven drugs identified as inhibitors in the screen, we determined K_i values using three concentrations of inhibitor, which spanned above and below the expected K_i based on the initial screening, across eight concentrations of azTolb. We then performed nonlinear least-squares regression of the Michaelis–Menten inhibition equations to determine the values of K_i for azTolb hydroxylation. The determined K_i values agree very well with values in the literature for the parent drug tolbutamide (Table 1), further validating the use of SAMDI for assaying drug metabolism and drug–drug interactions. Although we used a modified version of tolbutamide in our experiments, we found that all but one of the K_i values measured in this screen were within a factor of 2 of the previously reported values for tolbutamide. By contrast, fluorescent probes can result in IC_{50} values that vary by as much as 50-fold when compared to the unmodified drug substrates.⁵

Though the strategy presented here requires a modest chemical modification of the probe substrate, we have demonstrated for tolbutamide that the enzyme kinetics and drug–drug interactions for the probe substrate closely resemble those of the unmodified substrate. While this certainly would not apply to all drugs, there would be value even if it applied to only a fraction of drugs. This method would enable a comprehensive screening of approved drugs for potentially adverse interactions, a goal that is not readily achieved with current technologies. Furthermore, for drugs with moieties amenable to immobilization on monolayers with compatible capture chemistry, it may be possible to use this approach to assay unmodified drugs.

CONCLUSION

In conclusion, we have developed a SAMDI-based approach to assay the kinetics of drug metabolism and screen for drug–drug

interactions. We expect that this high-throughput method will enable characterization of the interactions of entire drug libraries with multiple probe substrates for each of the CYP450 isoforms, thereby screening drug–drug interactions at an unprecedented scale. This approach offers the potential to substantially increase our ability to anticipate drug–drug interactions and prevent adverse drug reactions.

ASSOCIATED CONTENT

Supporting Information

The Supporting Information is available free of charge on the ACS Publications website at DOI: 10.1021/acs.analchem.6b01750.

NMR spectra of azido-tolbutamide (PDF)

AUTHOR INFORMATION

Corresponding Authors

*E-mail: al.george@northwestern.edu.

*E-mail: milan.mrksich@northwestern.edu.

Author Contributions

[†]L.L.A. and E.J.B. contributed equally.

Notes

The authors declare no competing financial interest.

ACKNOWLEDGMENTS

This work was funded by the Defense Threat Reduction Agency (Grant HDTRA1-15-1-0052 to M.M.) and a Dixon Translational Research Grants Initiative. L.L.A. is the recipient of a postdoctoral fellowship grant from the PhRMA Foundation.

REFERENCES

- (1) Lazarou, J.; Pomeranz, B. H.; Corey, P. N. *JAMA, J. Am. Med. Assoc.* **1998**, *279*, 1200–1205.
- (2) White, T. J.; Arakelian, A.; Rho, J. P. *Pharmacoeconomics* **1999**, *15*, 445–458.
- (3) Crespi, C. L.; Miller, V. P.; Penman, B. W. *Anal. Biochem.* **1997**, *248*, 188–190.
- (4) Walsky, R. L.; Obach, R. S. *Drug Metab. Dispos.* **2004**, *32*, 647–660.
- (5) Crespi, C. L.; Stresser, D. M. *J. Pharmacol. Toxicol. Methods* **2000**, *44*, 325–331.
- (6) Danielson, P. B. *Curr. Drug Metab.* **2002**, *3*, 561–597.
- (7) Su, J.; Mrksich, M. *Angew. Chem., Int. Ed.* **2002**, *41*, 4715–4718.
- (8) Mrksich, M. *ACS Nano* **2008**, *2*, 7–18.
- (9) Gurard-Levin, Z. A.; Scholle, M. D.; Eisenberg, A. H.; Mrksich, M. *ACS Comb. Sci.* **2011**, *13*, 347–350.
- (10) Kuo, H. Y.; Deluca, T. A.; Miller, W. M.; Mrksich, M. *Anal. Chem.* **2013**, *85*, 10635–10642.
- (11) Schuster, T.; Schellenberger, S.; Friedrich, R.; Klapper, M.; Mullen, K. J. *Fluorine Chem.* **2013**, *154*, 30–36.
- (12) Landi, F.; Johansson, C. M.; Campopiano, D. J.; Hulme, A. N. *Org. Biomol. Chem.* **2010**, *8*, 56–59.
- (13) Houseman, B. T.; Gawalt, E. S.; Mrksich, M. *Langmuir* **2003**, *19*, 1522–1531.
- (14) Miners, J. O.; Birkett, D. J. *Br. J. Clin. Pharmacol.* **1998**, *45*, 525–538.
- (15) Presolski, S. I.; Hong, V. P.; Finn, M. G. *Curr. Protoc. Chem. Biol.* **2011**, *3*, 153–162.
- (16) Kumar, V.; Wahlstrom, J. L.; Rock, D. A.; Warren, C. J.; Gorman, L. A.; Tracy, T. S. *Drug Metab. Dispos.* **2006**, *34*, 1966–1975.
- (17) Ring, B. J.; Binkley, S. N.; Vandenbranden, M.; Wrighton, S. A. *Br. J. Clin. Pharmacol.* **1996**, *41*, 181–186.

- (18) Wen, X.; Wang, J. S.; Backman, J. T.; Kivisto, K. T.; Neuvonen, P. J. *Drug. Metab. Dispos.* **2001**, *29*, 1359–1361.
- (19) Komatsu, K.; Ito, K.; Nakajima, Y.; Kanamitsu, S.; Imaoka, S.; Funae, Y.; Green, C. E.; Tyson, C. A.; Shimada, N.; Sugiyama, Y. *Drug Metab. Dispos.* **2000**, *28*, 475–481.
- (20) Andersson, T. B.; Bredberg, E.; Ericsson, H.; Sjoberg, H. *Drug. Metab. Dispos.* **2004**, *32*, 715–721.
- (21) Wen, X.; Wang, J. S.; Kivisto, K. T.; Neuvonen, P. J.; Backman, J. T. *Br. J. Clin. Pharmacol.* **2001**, *52*, 547–553.
- (22) Furuta, S.; Kamada, E.; Suzuki, T.; Sugimoto, T.; Kawabata, Y.; Shinozaki, Y.; Sano, H. *Xenobiotica* **2001**, *31*, 1–10.
- (23) Lee, K. S.; Kim, S. K. *J. Appl. Toxicol.* **2013**, *33*, 100–108.